Modeling, Validation, and Design Investigation of a Passive Biped Walker with Knees and Biomimetic Feet

Aikaterini Smyrli*, *Student Member, IEEE*, and Evangelos Papadopoulos, *Fellow, IEEE*

Abstract— This paper studies a passive biped walker with knees and biomimetic feet and its behavior, as a function of key parameters. The model includes a continuous dynamic representation of the knee joint's interaction with a viscoelastic kneecap, as well as a complete kinematic description of feet that are designed to mimic the human rollover shape. First, the analytical model is derived and studied numerically for its passive walking capabilities. Then, the model is verified through independent simulations in a different platform. Finally, to increase the efficiency of its passive gaits and to map out its walking capabilities, the model is investigated parametrically. The methods used as well as the results obtained can offer significant assistance in the field of designing passivity-based biomimetic walking robots and prosthetic devices.

I. INTRODUCTION

The dynamics of human locomotion is a research field that has attracted the interest of roboticists over the years. In an effort to understand our species' optimal mode of locomotion, especially in terms of efficiency, several models of varying complexity have been suggested to date.

The first studies on bipedal walking were on simple, stiff-legged double-pendulum walkers, that were shown to have the ability to perform passive gait by successively bringing one pendulum-leg in front of the other, at each time preventing the walker's inverted pendulum fall [1][2][3]. Several variations of this biped walker, capable of passive walking, have been proposed to date.

The stiff-legged double pendulum walker approximates a human's gait but fails to account for the compliance observed in human walking, which is mainly due to the existence of multiple actuated joints. To overcome this challenge, some studies have introduced passive impedance elements such as springs and dampers, which were found to increase the biped walker's walking capabilities [4][5][6].

A more straightforward way of replicating the dynamic effects of knee compliance is the introduction of knee joints in the passive walker [7][8][9]. This increase in model complexity poses the significant challenge of synchronizing the various unactuated joints in a periodic motion. In some cases, some degree of under-actuation is introduced to enable a degree of manipulation of the kneed bipeds' dynamics [10][11]. Additionally to the compliance benefits, the kneed walker's passive ability to prevent foot scuffing has also been theoretically studied and utilized in manufactured robots [7][12][16][17] However, this knee joint compliance can

prove problematic in supporting the weight of the biped when the kneed leg is in contact with the ground, causing the biped to collapse. This possibility is affected by various parameters, such as mass distribution, initial velocities, and most importantly, the moment of the ground reaction forces with respect to the position of the knee joint axis [13]. Consequently, the type of foot the kneed biped walker is equipped with plays an important role in its ability to walk passively. To eliminate this problem, some constructed bipeds rely on securing the knee in a locked position, and make use of elements such as a passive suction cup [12] or an active locking device [14] [15].

Apart from its immediate effects on the ground reaction forces, the shape of the biped's feet also affects the overall compliance of the model [18]. Several studies have replaced the simple pointed feet of the early studied bipeds and incorporated more complex foot geometries, such as circular [19] or elliptic [20]. More recently, our team has worked on the incorporation of arbitrary foot geometries on the passive dynamics of a biped, and applied the developed methodology by introducing a human rollover footshape on a passive biped walker [21]. This biomimetic footshape effectively bypasses the active joints of the human foot, and leads to an ankle trajectory that is identical to the one recorded in human walking trials.

In this work, the model of a biped walker is developed, that includes passive knee joints with the addition of viscoelastic kneecaps, as well as the biomimetic footshape mentioned above. The viscoelastic kneecap enables a continuous representation of the knee's state, in contrast to previous studies which assumed a locked knee state in their simulations [7] or enforced it in their experiments [12] [14][15]. The biomimetic footshape is expected to contribute to the kneed biped's ability to perform fully passive gaits, as a benefit of the human-like ankle trajectory achievable through the rollover-shaped feet. The developed analytical model is simulated in MATLAB and studied for its ability to perform passive gaits. Additionally, the methods and model used are validated by an independently created solid model of the biped designed in the CAD software SolidWorks and simulated in the multibody dynamics platform MSC Adams. Following the model validation, a design study is performed, to identify parameter combinations of the biped model that lead to efficient gaits.

The modeling and simulation results of the biped model are presented in Section II. Section III presents the model validation process and Section IV analyzes the results of the design investigation. Finally, Section V concludes the study.

*Corresponding author.

The authors are with the School of Mechanical Engineering, National Technical University of Athens, (e-mail: katerinasmyrli@mail.ntua.gr, egpapado@central.ntua.gr, tel: +30 210-772-1440).

II. MODELING OF THE BIPED WITH KNEES

A. Model Description

The model that has been developed for the purposes of this study is shown in Fig. 1. It is comprised of four rigid links, each of which has mass and inertial properties, and joined together by three frictionless revolute joints: two at the knees and one at the hip of the biped. The hip joint is free to perform a full rotation; however, similarly to humans, the knee joints are constrained by viscoelastic kneecaps to prevent knee hyperextension.
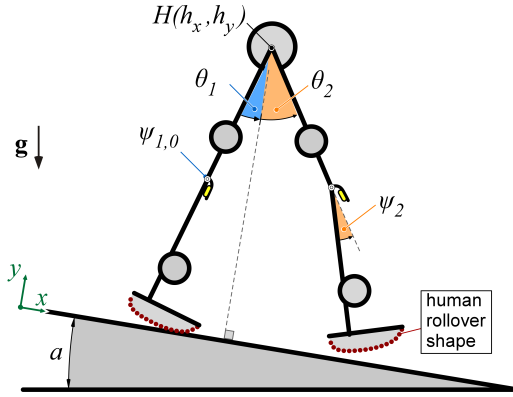

Fig. 1. The biped model used in this study, showing the model's generalized variables. The model includes teo legs with knees and biomimetic feet that mimic the human rollover shape. One of the legs of the model is in stance, where its knee angle has a value of $\psi_{1,0}$, and it is kept in position by the model's viscoelastic kneecap. The other leg is in swing and its knee is free to rotate.

The generalized coordinates of the model are the hip coordinates in the x-y plane, h_x and h_y respectively, the leg and knee angles for Leg 1, θ_1 and ψ_1, and the leg and knee angles for Leg 2, θ_2 and ψ_2. These comprise the generalized coordinates vector $\mathbf{q}$:

$$\mathbf{q} = [h_x, h_y, \theta_1, \psi_1, \theta_2, \psi_2]^{\mathrm{T}} \tag{1}$$

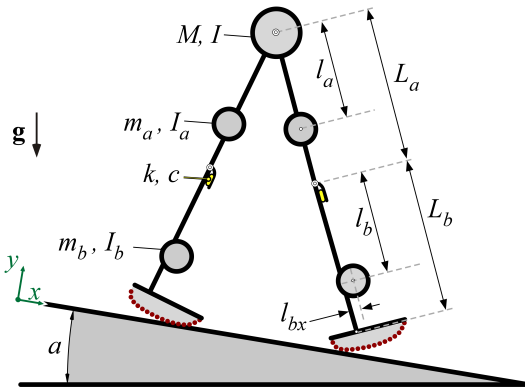The parameters of the model have been marked in Fig. 2.

Fig. 2. The biped model used in this study, showing the model's parameters. In this frame, both legs are in stance. The model's legs are symmetric, and the parameters are the same for both legs, but are only annotated on one to preserve diagram simplicity.

The biped is studied for its passive walk on a negative slope α, acting under the effect of the gravitational acceleration g. The inertial elements of the model are the hip mass M and moment of inertia I, and the point masses and moments of inertia of the leg segments, m_a and I_a for the upper limb sections (above the knee joints), and m_b and I_b for the lower limbs (below the knee joints). To account for the weight of the feet, the lower limb's center of mass is allowed an axial offset, symbolized as l_{bx}. The position of the leg segments' center of mass is defined by the positioning parameters l_a and l_b. Finally, the link lengths are also configurable by the parameters L_a and L_b.

The viscoelastic knee parameters are the knee stiffness k and knee damping c, as well as the knee angle at which the kneecap is met, $\psi_{1,0}$ for Leg 1 and $\psi_{2,0}$ for Leg 2. More specifically, the kneecap's viscoelastic stop is modelled as a branch function producing a force f_{ki}:

$$f_{ki} = \begin{cases} 0 & \psi_i < \psi_{i,o} \\ k(\psi_i - \psi_{i,0}) + c\dot{\psi}_i & \psi_i \geq \psi_{i,o} \end{cases} \tag{2}$$

Observation of (2) highlights that there is nothing to prevent the kneed leg from collapsing under the weight of the biped when in stance, except for the system's inertial forces. Therefore, the passive dynamics of the biped have to be such that the knee is forced in the direction that can be supported by the kneecap. The footshape of the biped is the design element that defines the biped's interaction with the ground, and therefore heavily affects the direction of the moments acting on the knee joint.

In this biped model, each leg is equipped with a biomimetic foot, to imitate the effect that a human foot has on knee functionality. The feet are modeled and implemented using a previously developed methodology [21], that allows the use of any set of points as a foot shape for the biped. In the current study, the feet have been assigned a geometry that matches the human rollover shape, leading to an ankle trajectory that mimics the one observed in human walking trials [21].

B. Phases of Walking

Each leg of the biped can either be in contact with the ground and be subjected to the Ground Reaction Forces (GRFs), or be above the ground and not subject to any external forces. Most of the time during walking, a biped will have one leg in contact with the ground in a *stance* phase, while the other will be in a *swing* phase above the ground. For a short time during a walking cycle, a biped walker will have both its legs in a double stance phase.

One of the legs of the biped in Fig. 1 is in stance: it acts as an inverted pendulum and the corresponding knee remains fully extended as the kneecap's stiffness prevents the knee's hyperextension. However, as previously mentioned, the knee is free to collapse in the other direction, and therefore it is essential that the moments acting on the stance leg's knee are in the direction that compresses the kneecap. The other leg is in *swing*: it acts as a double pendulum and it is therefore brought passively forward due to its inertial

properties. During the swing leg's forward advancement, the corresponding knee might passively fold for certain inertial distributions: in fact, this is desirable as -if properly synchronized- it can prevent the foot from scuffing the ground. Towards the end of its swing phase, the swing knee will extend until it hits the kneecap, in an event called *Knee Strike* (KS). At the same time, the swing leg approaches the top of its pendulum trajectory, after which it stops and retracts towards its equilibrium position. At this stage, it is desirable to synchronize the swing leg's retraction with its knee's extension, so that when the foot hits the ground at *Heel Strike* (HS), the impact keeps the knee extended.

When only one of the legs is in stance phase, then the biped is said to be in a *Single Stance Phase* (SSP), see Fig. 1. After a HS event, the biped enters a *Double Stance Phase* (DSP), during which both legs are in contact with the ground, see Fig. 2. The DSP ends when the GRFs acting on either leg drop to zero, in an event called *Toe Off* (TO), after which a new SSP commences.

The biped's passive dynamics differ between a SSP and a DSP, and therefore the biped model is categorized as a nonlinear, hybrid system. An analytical solution for this type of system does not exist, and numerical approaches are employed in its dynamics' study. In the next sections, the dynamic model for this system is described.

C. Passive Body Dynamics and Foot Kinetics

A key objective in designing walking robots is gait efficiency. To achieve an efficient gait, the energy required to perform a walk must be minimized. This requirement is met by robots that are capable of passive gaits in small negative slopes. The existence of a passive repetitive gait cycle implies that the energy expenditure of the walk per unit distance is equal to the sine of the slope angle [20], which is small when the angles are small. Moreover, there is no actuation cost in a passive motion. Additionally, gait stability ensures that there is no need for trajectory corrective action, as the dynamics naturally converge towards a stable gait. Therefore, the quest for gait efficiency usually leads to the study of *stable passive* dynamics.

To facilitate the analytical model description, the model is divided in two parts: the first part includes the *dynamic components* in the form of differential equations, while the second one consists of the *kinematic constraints* that apply to the rolling contact of the feet with the ground, in algebraic form. More specifically, the dynamics of the biped model are derived using the Lagrangian formulation. The kinematic constraints acting on the biped are dependent on the foot geometry. In short, during its contact with the ground, a foot must satisfy a set of 2 kinematic constraints to avoid both the slipping and the sinking motion with respect to the ground. These constraints have been formulated in numerical form for any type of convex foot shape and the developed methodology has been presented in [21]. In this study, there are two constraints for each leg, which are activated when the leg is in stance. Therefore, for the biped's two legs, the constraint vector, s, is 4x1.

The equations of motion are of the general form:

$$\mathbf{M(q)\ddot{q}} + \mathbf{C(q,\dot{q})\dot{q}} + \mathbf{K(q)} + \mathbf{G(q)} - \mathbf{f} = 0$$
$$\mathbf{Ws(q)} = 0 \tag{3}$$

In (3) $\mathbf{M}$ is the 6x6 system inertia matrix, $\mathbf{C}$ is a 6x1 vector containing Coriolis, centrifugal and damping terms, and $\mathbf{K}$ and $\mathbf{G}$ are the 6x1 stiffness and gravity force vectors respectively. The matrix $\mathbf{W}$:

$$\mathbf{W} = \mathrm{diag}(w_1, w_1, w_2, w_2) \tag{4}$$

is a 4x4 square diagonal *switching* matrix where $w_i = 0$ when leg-i is in swing and $w_i = 1$ when it is in stance. Effectively, $\mathbf{W}$ activates the application of the kinematic constraints $\mathbf{s} = 0$ to constrain each leg in rolling motion on the ground when in stance phase. Finally, $\mathbf{f}$ is a constraint force vector, also a function of the switching matrix $\mathbf{W}$:

$$\mathbf{f} = \left(\frac{\partial(\mathbf{Ws})}{\partial \mathbf{q}}\right)^{\mathrm{T}} \boldsymbol{\lambda} \tag{5}$$

where $\boldsymbol{\lambda}$ is the 4x1 Lagrange multiplier vector containing the GRF components that correspond to the constraints in $\mathbf{s}$.

Observation of (3) and (5) highlights the dependence of the system of equations on the number of legs in contact with the ground at each time step. When both legs are in stance, then $\mathbf{W}$ is equal to the 4x4 identity matrix, and the system in (3) is a Differential Algebraic Equation (DAE) system, comprised of a set of 6 second-order Ordinary Differential Equations (ODEs) and 4 Algebraic Constraints (ACs) that must be satisfied by the system solution. When the i-th leg is in swing phase, then $w_i = 0$ and the ACs acting on the DAE system are reduced to 2. In bipedal walking, there is no instance when both legs are in swing.

The latter observation leads to the conclusion that at all times, at least 2 of the biped's DoFs are constrained, and therefore the elements of $\mathbf{q}$ are not fully independent. In fact, the temporal propagation of the coordinates h_x and h_y is a function of the rest of the generalized coordinates in $\mathbf{q}$: it is the ACs that define this dependence. Therefore, the vector that minimally describes the state $\mathbf{x}$ of the biped is:

$$\mathbf{x} = [\theta_1, \psi_1, \theta_2, \psi_2, \dot{\theta}_1, \dot{\psi}_1, \dot{\theta}_2, \dot{\psi}_2]^{\mathrm{T}} \tag{6}$$

Note that the size of $\mathbf{x}$ is 8x1. Even though some of the generalized variables are not needed in $\mathbf{x}$, they cannot be emitted from the system description, as they are required in the DAEs of (3) to ensure that the appended constraints are satisfied. For some DAE systems it is possible to solve the ACs for the constrained variables and to substitute their value in the ODEs, eliminating them altogether and reducing the system's order and complexity. Unfortunately, this method is not practical for the system under study, due to the nonlinearity of the constraints. Therefore, the system can only be simulated using a special class of solvers that can handle DAE systems.

D. Simulation and Periodic Gaits

In MATLAB, the solvers capable of handling DAEs are ode23t and ode15s. The latter has been selected for this study, as it is more suitable for stiff system dynamics.

The model is simulated for its response to Initial Conditions (ICs) $\mathbf{x_0}$. In a *periodic* gait, the state will be repeated after a full step of the biped. In this work we are interested not only in the existence of periodic gaits, but also in their stability characterization. A periodic gait will theoretically map back on the same state infinite times; however, small state variations caused by disturbances in physical systems or even noise in simulations, will result in dynamic divergence if the gait is not stable. On the other hand, for initial states around a *stable* periodic orbit, the dynamics converge towards the periodic gait, and therefore any disturbances in the system's state are rejected. Details about the numerical identification and stability characterization of periodic gaits in biped models can be found in our previous work [6] and [20] and will be spared here. Fig 3 presents frames of the biped's stable periodic gait, as simulated in MATLAB.
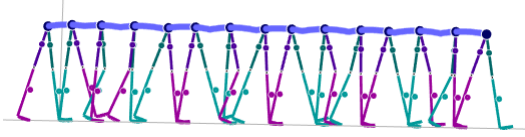

Fig. 3.   Stable periodic gait progression of the biped in MATLAB.

Fig. 4 presents a projection of a periodic orbit of the biped's dynamics, on the phase plane of Leg 1's angles for 10 consecutive steps. The leg and knee angles, θ_1 and ψ_1, are plotted in the two graphs, (a) and (b) respectively. The chart should be read in a clockwise direction.
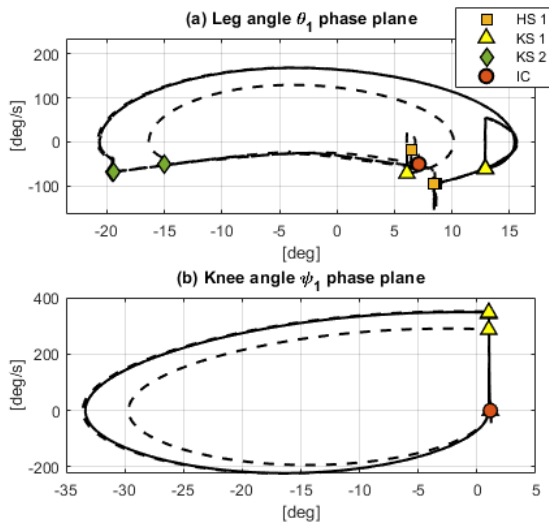

Fig. 4.   Phase plane for the leg (a) and knee (b) angles of one leg of the biped, for 10 consecutive steps, beginning from ICs outside the stable periodic gait trajectory and converging towards it. The graphs are plotted using a dashed line: when the dynamics converge in the periodic trajectory after 2 steps, the lines are overlaid, appearing as solid, continuous curves.

The ICs of the simulation lie outside the stable periodic state trajectories; consequently, the stability of the selected gait is evidenced in Fig. 4 by the convergence of the dynamics towards the periodic gait trajectory in both graphs.

A dashed line has been selected for the plots, to distinguish between the transient convergent response and the stable periodic trajectory, at which many dashed lines are overlaid and appear as solid.

Fig. 4 also shows a selection of key events that occur during a step of the biped: these are the Leg 1 HS and KS as well as the Leg 2 HS. It can be observed that there is a vertical jump in the angle velocities after a HS or KS event. This is due to the impact experienced by the biped's DoFs at first contact. Additionally, it is important to note that due to the knees' stiffness, the DSP is short: the TO event would be indistinguishable from the corresponding HS, and it is therefore emitted.

Please note that the parameters of the biped model in these simulations are marked with a blue square and their values have been tagged at the design maps of Section IV.

III. Model Validation

The simulation of the biped in MATLAB is based on the analytical description of the system dynamics in (3) and could be subject to modeling errors, coding bugs or even misrepresentation of the dynamic behaviour due to unsuitability of the selected solver. To ensure that none of the above significantly affect the reliability of results obtained, the simulation is independently reproduced using MSC Adams and the results are be compared.

A. Modeling in MSC Adams vs MATLAB

MSC Adams is a multibody simulation environment where solid bodies can be combined to form a multibody system, which can be simulated for its response under various loads and/or ICs. The bodies can be directly imported from CAD programs, facilitating the design process. MSC Adams has been utilized for validation of simpler walking models, without knees and with simple circular feet, producing encouraging results [22]. Therefore, its use in the validation of the kneed biomimetic walker is expected to indicate the validity of the newly introduced attributes of the walker: its viscoelastic knees and rollover-shaped feet, as well as their dynamic cooperation.

For this study, a solid model of the biped was designed in SolidWorks and imported in MSC Adams. The model can be observed in Fig. 5. The parameters of the solid model are set equal to the parameters of the analytical model that was studied in MATLAB. The initial conditions given to the two models are also the same.

A significant difference between the MATLAB and MSC Adams models is the modeling of the feet's contact with the ground. In MATLAB, Lagrangian constraints have been selected to model the rolling motion of the feet on the ground. This modeling has been presented in [21], and it includes a numerical representation of the footshape's geometric attributes and of its interaction with the ground. While the
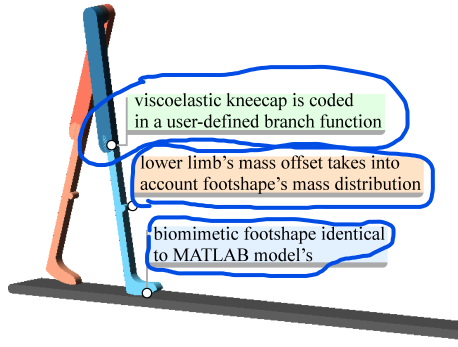
Fig. 5. The biped model in MSC Adams, as imported from SolidWorks, in its initial configuration. The model parameters as well as ICs of the MSC Adams model are identical to the ones of the MATLAB model. Therefore, dynamic resemblance between the two models' responses is expected.
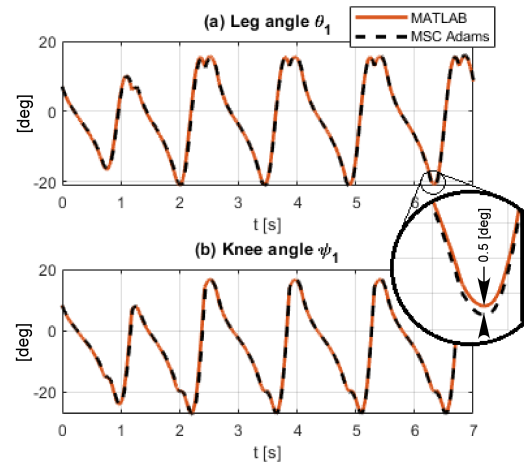

Fig. 6. Comparison of the MATLAB and MSC Adams dynamic responses. The two models' behaviour is almost identical. The maximum divergence is 0.5 [deg] and it is shown in detailed view.

methodology has been validated through comparisons using simple foot shapes, such as a point or an ellipse, no validation has been performed for more complex footshapes, for which an analytical expression does not exist. By designing the custom footshape in SolidWorks and simulating it in MSC Adams, a completely independent approach is followed. MSC Adams has a dedicated contact function, that uses a viscoelastic contact model for the normal ground force, and a Coulomb model for the frictional force. Despite the modeling differences, the two approaches have been found to produce equivalent results in simpler biped models [22].

Additionally, MSC Adams offers its own selection of solvers, which is different from the ones available in MATLAB. Similarly to the solver selection in MATLAB, a stiff solver is preferred here as well. The simulation in MSC Adams is performed using the GSTIFF solver under the "Dynamics" simulation option. This solver has also been proven reliable for simulations of the simpler biped models previously mentioned [22].

The above are the most common occurrences of dynamic divergence between the different simulation platforms. A high degree of dynamic resemblance between the two models will validate the modeling of the biped, especially with respect to the novel attributes of the walker that have not been cross-validated to date.

B. Comparison and Validation of Results

The MSC Adams model is simulated for its passive gait, using an educated guess for its parameter set and initial conditions, indicated by the study previously performed in MATLAB. The MSC Adams biped performs a repetitive gait that is presented in Fig. 6 along with the corresponding data from the MATLAB simulation.

The comparison plots present the responses of the passive bipeds in MATLAB and MSC Adams to identical ICs outside the stable periodic gait trajectory: these are the same initial conditions that have been previously used in the phase plane plots of Fig. 5. Fig. 6(a) presents the Leg 1 angle θ_1 and Fig. 6(b) presents the corresponding knee angle ψ_1. Both charts present an initial transient response before their convergence to repetitive trajectories. The MATLAB results are plotted

using an orange solid line, while the MSC Adams results are presented in a black dashed line. The two responses are almost identical, and only differ slightly. The maximum difference of the two responses is 0.5 [deg], shown in the detailed view of Fig. 6. This difference can be attributed to the different modeling of the ground contact, as previsouly mentioned.

The high degree of dynamic resemblance between the two models indicates that the analytical modeling of the biped's knees and biomimetic footshape has been performed correctly, and that the MATLAB simulation yields accurate and reliable results.

Since the two simulation methods produce the same results, either one might be used for parameter investigation studies. The MATLAB model is more configurable and facilitates changes in parameter values; while the MSC Adams simulation needs a lot of time to setup, especially since the solid model has to be created in CAD, imported and configured before it can be simulated. Additionally, the simulation run time in the MATLAB model is significantly shorter than for its MSC Adams counterpart, for the same result accuracy. Therefore, the MSC Adams model is only utilized here for the validation of the MATLAB simulations, which will be subsequently used to investigate the model design.

IV. Design Investigation

The MATLAB model that has been developed and verified in the previous sections will be used in this section to derive a set of design maps, to investigate the parameter ranges for which efficient gaits exist.

It has been shown that the Cost of Transport of passive gaits on a negative slope α is equal to [20]:

$$COT = \frac{\text{energy spent}}{\text{(biped's weight)(distance travelled)}} = \sin(\alpha) \quad (7)$$

The main motivation in studying passive walkers is energy efficiency and therefore minimization of COT. Consequently, we are mainly interested in gaits that are achievable in small negative slopes α, as these could theoretically be replicated on level ground with a small energy expenditure. For this reason, the design investigation in this study focuses on the slope values for which passive gaits exist, while the rest of the model's parameters are swiped within a predetermined range.

Fig. 7 presents the design investigation results in graphical form. For each of the plots (a) - (l) one of the model's parameters, plotted along the x-axis of each graph, is swiped within its allowed range. For each value of this parameter, the range of slope angles for which a stable passive gait exists is identified. This process results in the yellow regions of Fig. 7, which map the efficient walking capabilities of the biped as its parameters change. The purple regions are combinations for which stable passive gaits do not exist: these generally enclose the yellow regions and mark the outlines of the efficient walking design region. Finally, the blue square in each plot shows the *nominal* parameter value for the biped, which is the one that has been used for the study and validation of the model in the previous sections. The tags mark these nominal values. This set has been selected for its ability to walk on a very small slope $\alpha = -2.6$ [deg], which translates to a COT = 0.045, which lies within the estimated range of the human walking COT [23].

Observation of Fig. 7 indicates that for most parameters, there is a large range of parameter values for which stable passive gaits can be performed. These parameters are the masses and lengths of the model, in plots (a) - (f). However, the biped model appears to be especially sensitive to variations in its limb's moments of inertia, I_a in plot (i) and I_b in plot (j). Another parameter that appears to affect the biped's ability to perform efficient passive gait is the lower leg mass offset, l_{bx}, which indicates the dependence of the results on the footshape of the biped. On the other hand, the hip's moment of inertia, I in plot (h), does not affect the biped at all, as it is designed to be located on the hip axis which rotates freely.

The knee dynamics, configured by parameters k in plot (k) and c in plot (l) also have a significant effect on the biped's ability for passive walking on various slopes. For small k values, the biped only has a small range of slopes on which it can passively walk. This range increases once the stiffness k surpasses 500 [Nm/rad] or when the damping c goes below 10 [Nms/rad]. Therefore, stiffer knees with smaller damping allow for a wider range of walking modes.

Before concluding the study, it is important to note that the plots of Fig. 7 reveal another insight about the biped model: for some plots, such as the upper and lower leg's moments of inertia I_a and I_b in plots (i), (j) and the knee stiffness k in plot (k), there appears to exist more than one ways to walk, as for some parameter values a vertical line would cross the map twice, once for a small α value and therefore a small slope, and once for a steeper slope. This is an instance of bifurcations of the passive biped's nonlinear dynamics.
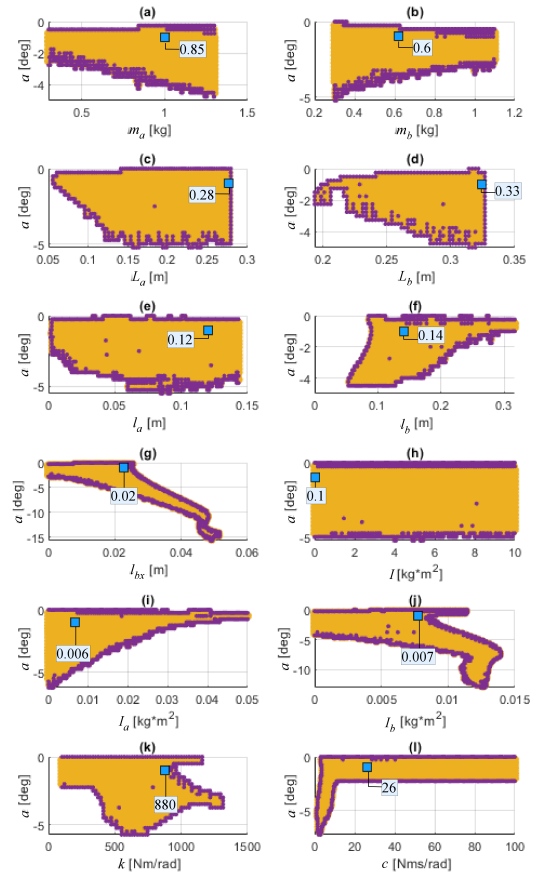

Fig. 7. Parameter investigation for the verified MATLAB biped model. The x-axis of each graph corresponds to one of the model's parameters. The y-axis of all graphs corresponds to slope a. The yellow region shows the parameter values for which stable passive gait exists. For the purple regions, the biped does not exhibit stable passive gait. The blue square shows the nominal parameters on the map, while the tag notes their exact value (the tag's units are those of the x-axis).

V. Conclusion

In this study, the analytical model of a biped with knees and biomimetic feet has been developed, validated and used in an efficiency-oriented design investigation. The developed model has been proven to be accurate and reliable in the prediction of the biped's passive dynamic behaviour, through comparison of the results obtained via its numerical simulation in MATLAB, to a completely independent model description and simulation, performed by the multibody dynamics simulation package MSC Adams. This validation is significant, since the analytical model incorporates a set of dynamic and kinematic elements that have not been used cooperatively or validated in the past, such as the viscoelastic kneecaps and the biomimetic footshapes. The validated model was then utilized to create design investigation maps, focused on identifying parameter combinations that produce a biped able to walk on many different slopes, which translates to many different energetic efficiency levels. The resulting design maps can be utilized with confidence in the design of kneed biped robots for experimental studies of passive walking, which is the next step in our future work.

REFERENCES

[1] McGeer, T., "Passive Dynamic Walking," *The International Journal of Robotics Research*, 1990, 9(2): pp. 62-82.

[2] Garcia, M., et al., "The Simplest Walking Model: Stability, Complexity, and Scaling," *Journal of Biomechanical Engineering*, 1998, 120(2): pp. 281-288.

[3] Espiau, B., and Goswami, A., "Compass gait revisited," *IFAC Proceedings Volumes*, 1994, 27(14): pp. 839-846.

[4] Alexander, R., "A model of bipedal locomotion on compliant legs," *Philosophical Transactions of the Royal Society of London, Series B: Biological Sciences*, 1992, 338(1284): pp. 189-198.

[5] Linde, R.Q.V.D., "Active leg compliance for passive walking," *IEEE International Conference on Robotics and Automation (ICRA '98)*, Leuven, Belgium, 1998, pp. 2339-2344.

[6] Smyrli, A., Bertos, G. and Papadopoulos, E., "Efficient stabilization of zero-slope walking for bipedal robots following their passive fixed point trajectories," *IEEE International Conference on Robotics and Automation (ICRA '18)*, Brisbane, Australia, 2018, pp. 5733-5738.

[7] McGeer, T., "Passive walking with knees," *IEEE International Conference on Robotics and Automation (ICRA '90)*, Cincinati, OH, USA, 1990, pp. 1640-1645

[8] Owaki D., Koyama M., Yamaguchi s., Kubo s. and Ishiguro a., "A two-dimensional passive dynamic running biped with knees," *IEEE International Conference on Robotics and Automation*, Anchorage, AK, 2010, pp. 5237-5242.

[9] Moon J., Lee S., Bae J. and Youm Y., "Analysis of period-1 passive limit cycles for flexible walking of a biped with knees and point feet". *Robotica*, 2016, 34(11): pp. 2486-2498.

[10] Hamon, A. and Aoustin, Y., "Study of different structures of the knee joint for a planar bipedal robot," *IEEE-RAS International Conference on Humanoid Robots*, Paris, France, 2009, pp. 113-120.

[11] Harata, Y., Asano, F., Luo, Z., Taji, K. and Uno Y., "Biped gait generation based on parametric excitation by knee-joint actuation," *IEEE/RSJ International Conference on Intelligent Robots and Systems (IROS '07)*, San Diego, CA, 2007, pp. 2198-2203.

[12] Collins S. H., Wisse, M., and Ruina, A., "A three-dimensional passive-dynamic walking robot with two legs and knees," *The International Journal of Robotics Research*, 2001, 20(7): pp. 607–615.

[13] Radcliffe, C. W., "Four-bar linkage prosthetic knee mechanisms: Kinematics, alignment and prescription criteria," *Prosthetics and Orthotics International*, 1994, 18(3): pp. 159-173.

[14] Collins, S. H. and Ruina, A., "A Bipedal Walking Robot with Efficient and Human-Like Gait," *IEEE International Conference on Robotics and Automation (ICRA '05)*, Barcelona, Spain, 2005, pp. 1983-1988.

[15] G. van Oort, R. Carloni, D. J. Borgerink and S. Stramigioli, "An energy efficient knee locking mechanism for a dynamically walking robot," *IEEE International Conference on Robotics and Automation (ICRA '11)*, Shanghai, China, 2011, pp. 2003-2008.

[16] Mochon, S., and McMahon, T. A., "Ballistic Walking: An Improved Model," *Mathematical Biosciences*, 1980, 52(4-3): pp. 241–260.

[17] Ikemata, Y., Yasuhara, K., Sano, A. and Fujimoto, H., "A study of the leg-swing motion of passive walking," *IEEE International Conference on Robotics and Automation (ICRA '08)*, Pasadena, CA, 2008, pp. 1588-1593.

[18] Gard, S.A. and Childress, D.S., "What Determines the Vertical Displacement of the Body During Normal Walking?," *Journal of Prosthetics and Orthotics*, 2001, 13(3): pp. 64-67.

[19] Asano, F. and Luo, Z.W., "The effect of semicircular feet on energy dissipation by heel-strike in dynamic biped locomotion," *IEEE International Conference on Robotics and Automation (ICRA '07)*, Rome, Italy, 2007, pp. 3976-3981.

[20] Smyrli, A., Ghiassi, M., Kecskeméthy, A. and Papadopoulos, E. "On the effect of semielliptical foot shape on the energetic efficiency of passive bipedal gait," *IEEE/RSJ International Conference on Intelligent Robots and Systems (IROS '19)*, Macau, China, 2019, pp. 6302-6307.

[21] Smyrli, A. and Papadopoulos, E., "A methodology for the incorporation of arbitrarily-shaped feet in passive bipedal walking dynamics," *IEEE International Conference on Robotics and Automation (ICRA '20)*, Paris, France, 2020, pp. 8719-8725.

[22] Vasileiou, C., Smyrli, A., Drogosis, A. and Papadopoulos, E., "Development of a passive biped robot digital twin using analysis, experiments, and a multibody simulation environment," *Mechanism and Machine Theory*, 2021, 163, 104346.

[23] Donelan, J. M., Kram, R. and Kuo, A. D., "Mechanical Work for Step-to-Step Transitions is a Major Determinant of the Metabolic Cost of Human Walking," *Journal of Experimental Biololy*, 2002, 205(23): pp. 3717–3727.